# Thermoelastic intermartensitic transformation and its internal stress dependency in $Ni_{52}Mn_{24}Ga_{24}$ single crystals

W. H. Wang, Z. H. Liu, J. Zhang, J. L. Chen, G. H. Wu,* and W. S. Zhan
*State Key Laboratory for Magnetism, Institute of Physics, Chinese Academy of Sciences, P.O. Box 603, Beijing 100080, People's Republic of China*

T. S. Chin
*Department of Materials Science and Engineering, Tsing Hua University, Hsinchu, 30043, Taiwan, China*

G. H. Wen and X. X. Zhang
*Department of Physics, The Hong Kong University of Science and Technology, Clear Water Bay, Kowloon, Hong Kong, People's Republic of China*

(Received 7 January 2002; revised manuscript received 25 March 2002; published 12 August 2002)

We have found a *perfect thermoelastic* intermartensitic transformation between the seven-layer modulation ($7M$) and the five-layer modulation ($5M$) martensites in an unstressed $Ni_{52}Mn_{24}Ga_{24}$ single crystal. In particular, we found that the intermartensitic transformation is very sensitive to the internal stress built up during the grinding process. Based on our calculation, an average internal stress of $13.8 \pm 1.08$ MPa stored in the distorted lattice will force the parent phase to take a totally different martensitic transformation path during cooling and results in the entire suppression of the intermartensitic transformation. These results can be interpreted in terms of the formation of a $5M$ martensite which is facilitated by the elastic deformation.

DOI: 10.1103/PhysRevB.66.052411 PACS number(s): 64.70.Kb, 81.30.Kf, 75.50.Cc

The recent discovery of the large magnetic-field-induced strain[1–3] and magnetic-field, controllable shape memory behavior[4,5] in the ferromagnetic Heusler alloy $Ni_2MnGa$ has triggered great interest in the field of shape memory alloys. Immediately, the related physical mechanisms of these large recoverable strains have been intensively investigated accompanied by the martensitic transformation by many groups.[6–10] All these works indicate that $Ni_2MnGa$ is a very promising material for applications in high sensitivity magnetic sensors and actuators. In addition to the martensitic transformation, an intermartensitic transformation also exists in alloys with the martensitic transformation temperature $T_M$ near or higher than room temperature. Previous investigations[11,12] have verified that the intermartensitic transformation is a first-order phase transformation between martensites with different structures at temperatures $T_I$, where $T_I < T_M$. So far, several intermartensitic phases have been found, which have a modulated lattice with different periodicity of stacking sequences along the $\langle 110 \rangle_P$ direction (the subscript $P$ denotes the parent phase). Their structures and transformation temperatures $T_I$ depend on the levels of applied stress and the chemical composition. Earlier work by Martynov and Kokorin has established[11] that two successive intermartensitic transformations concerned with five-layer modulation martensite (termed in the literature $5M$), seven-layer modulation martensite ($7M$), and unmodulated martensite ($T$) can be induced from the parent phase ($P$) by increasing external stress at temperatures above $T_M$, with a sequence of $P \rightarrow 5M \rightarrow 7M \rightarrow T$. Recently, thermally induced *nonthermoelastic* intermartensitic transformations from $8M$ to $T$ or from $10M$ to $7M$ (depending on the composition) have been found by Chernenko *et al.*[13] in some samples richer in Mn.

In this paper we report the discovery of a *perfect thermoelastic* intermartensitic transformation between $7M$ and $5M$ martensites in an unstressed single crystal of $Ni_{52}Mn_{24}Ga_{24}$. The characteristic structures of $5M$ and $7M$ martensites have been determined. We found that the thermoelastic intermartensitic transformation in this material is very sensitive to the internal stress. Based on our calculation, a small average internal stress of $13.8 \pm 1.08$ MPa stored in the distorted lattice will force the parent phase to take a totally different structural path during the martensitic transformation and result in the preferential formation of a $5M$ martensite. This implies that a low-energy transformation path between the parent phase and the $5M$ martensitic phase is created to relieve the internal stress in samples. Experimentally such an influence relating to the internal stress has never been investigated in Ni-Mn-Ga crystals.

Single crystals of $Ni_{52}Mn_{24}Ga_{24}$ were grown in the [001] direction of the cubic parent phase by a MCGS-3 CZ (Czochralski) instrument with a cold crucible system. The grown rates of $12 \sim 15$ mm/h and rotation rate of 30 rpm were adopted. As-grown crystals were annealed at about 800°C for 24 h for high chemical ordering, then cooled to 500 °C quickly by compressed air and then annealed at this temperature again for 24 h to eliminate disordering residual stress caused by the quick cooling. Samples for electric resistivity and magnetic-susceptibility measurements were spark cut from the as-treated single-crystal rod. Electrical resistivity was measured by a standard four-probe technique in a zero magnetic field with a heating/cooling rate of 1 K/min. The magnetic-susceptibility measurement was performed by an ac susceptometer with an ac magnetic field of 5 Oe and a frequency of 77 Hz over a temperature range 77–400 K. Part of the $Ni_{52}Mn_{24}Ga_{24}$ single crystal was crushed into particles

 

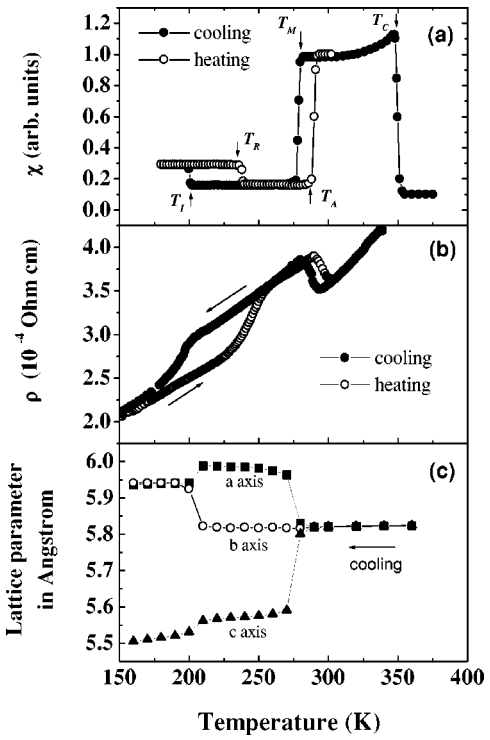


FIG. 1. Temperature dependence of (a) the ac magnetic susceptibility, (b) the electrical resistivity measured with the current along the [001] direction in the absence of a magnetic field, and (c) the lattice parameters for a $Ni_{52}Mn_{24}Ga_{24}$ single crystal. The Curie temperature $T_C$, the forward martensitic and intermartensitic transformation temperatures $T_M$ and $T_I$, and the reverse intermartensitic and martensitic transformation temperatures $T_R$ and $T_A$, are marked by the arrows, respectively.

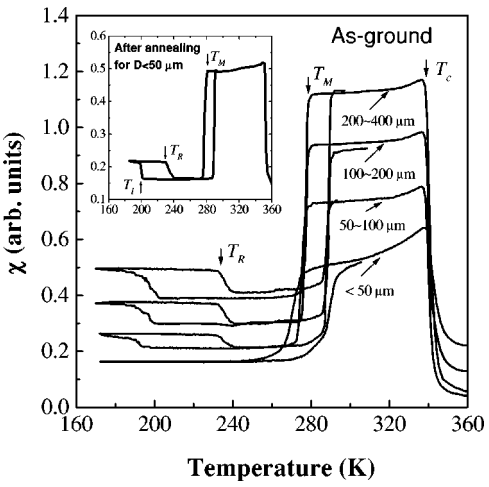


FIG. 2. Temperature dependence of ac magnetic susceptibility for the as-ground powder samples with varying particle size *D*. All the powder samples were first heated up to 400 K, and then cooled down to 100 K. Inset: Temperature dependence of ac magnetic susceptibility for the powder sample with $D<50$ $\mu$m after annealing at 500 °C for 10 h.

at room temperature, and ground into powders with four specific particle sizes, i.e., 200–400 $\mu$m, 100–200 $\mu$m, 50–100 $\mu$m, and less than 50 $\mu$m, respectively. Powder x-ray diffraction (XRD) was performed by a low-temperature diffractometer (Philip-Pert's MPD). Intensity data were collected with Cu $K\alpha$ radiation over a $2\theta$ range from 30° to 90° at a step width of 0.02°. In order to obtain the precise structural information from the XRD examination, ground powder samples with a size less than 50 $\mu$m were carefully annealed for 10 h at 500 °C in vacuum to eliminate the internal stress built up during severe grinding.

Figure 1 shows the temperature dependence of the ac magnetic susceptibility ($\chi$), the electrical resistivity ($\rho$), and the lattice parameters of the $Ni_{52}Mn_{24}Ga_{24}$ single crystal. As a generic feature of ferromagnetic material, the crystal undergoes a ferromagnetic transition at the Curie temperature $T_c=350$ K as marked by an arrow in the $\chi$-$T$ curve. Upon cooling, a sharp down jump occurs in the $\chi$-$T$ curve at $T_M=286$ K, which is in accordance with a pronounced upturn at 286 K in the $\rho$-$T$ curve of Fig. 1(b), revealing the martensitic transformation. With further decrease in temperature, another abrupt increase of $\chi$ occurs at $T_I=202$ K, and correspondingly, the resistivity shows a downturn at 202 K. It indicates that another distinct structural transformation, namely, the intermartensitic transformation, occurs at $T_I$ in our sample. On subsequent heating up to $T_R=240$ K, a down jump in the $\chi$-$T$ curve (corresponding to an upturn at 240 K in the $\rho$-$T$ curve) indicates the reverse intermartensitic transformation. In accordance with these changes in magnetic and electric properties, the lattice parameters also show a distinct change at both $T_M$ and $T_I$. As depicted in Fig. 1(c), the parent phase of our sample shows a cubic $L2_1$ structure (space group $Fm\bar{3}m$) with lattice parameters $a=b=c=5.824$ Å, in good agreement with the values reported in Ref. 11. Upon cooling down to $T_M$, an orthorhombic martensitic phase (space group $Fmmm$) is obtained due to the martensitic transformation with the following lattice parameters: $a=5.982$ Å, $b=5.817$ Å, and $c=5.572$ Å. By further cooling down to $T_I$, the intermartensitic transformation occurs and the orthorhombic martensite transforms again to a tetragonal one (space group $I_4/mmm$). The lattice parameters are $a=b=5.940$ Å, $c=5.530$ Å.

Based on the structure of the stress-induced martensite studied by *in situ* XRD in Ref. 11, and on our structure examinations above, we confirm that the intermartensitic transformation occurring in our sample is between $7M$ and $5M$ martensites. Clearly, this transformation observed in our sample shows a *perfect thermoelastic behavior*, viz., both the forward ($7M\rightarrow5M$) and the backward ($5M\rightarrow7M$) intermartensitic transformations can be obtained unequivocally at $T_I=202$ K (cooling) and $T_R=240$ K (heating), respectively.

In addition, we found that the intermartensitic transformation shows a strong internal stress dependency. In the as-ground powder sample with a particle size less than 50 $\mu$m without further annealing at 500 °C, the $7M\rightarrow5M$ transformation could not be detected by our magnetic measurements. Figure 2 shows the $\chi$-$T$ curves of the as-ground powder samples with various particle sizes. It is noticeable that the extent of $7M\rightarrow5M$ transformation is gradually suppressed as the single-crystal sample is ground to smaller and smaller

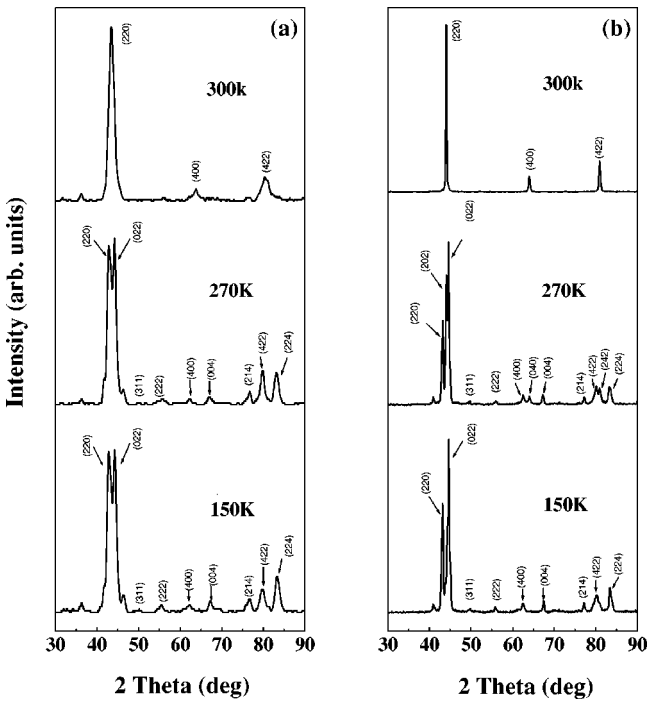


FIG. 3. X-ray-diffraction patterns of the as-ground powder sample with $D<50$ $\mu$m (a) before annealing and (b) after annealing at 500 °C for 10 h at various temperatures.

particle sizes. When the as-ground powder sample reaches a particle size less than 50 $\mu$m, the $7M \rightarrow 5M$ transformation disappears completely. Subsequently, when the as-ground powder sample ($D<50$ $\mu$m) was annealed at 500 °C for 10 h in vacuum to completely eliminate the internal stress buildup during the grinding process, the $7M \rightarrow 5M$ transformation was restored (see the inset in Fig. 2).

In order to verify the magnetic-susceptibility results, x-ray powder-diffraction measurements were performed at different temperatures. In this way, we can determine in more detail the structural evolution of the as-ground and the annealed powder samples ($D<50$ $\mu$m). Figure 3 shows XRD patterns taken at $T=300$, 270, and 150 K, respectively. All the intense peaks have been indexed and marked in Fig. 3. One can see that, in the parent phase (300 K), both the as-ground and the annealed powder samples show a cubic structure with three characteristic reflection peaks $(220)_{cubic}$, $(400)_{cubic}$, and $(422)_{cubic}$. On cooling down to 270 K, just below $T_M$, the XRD patterns of both the as-ground and the annealed powder samples reveal a remarkable change. For the annealed one, the $(220)_{cubic}$ peak, for example, splits into three peaks, i.e., $(220)_{orth}$, $(202)_{orth}$, and $(022)_{orth}$, respectively. [For simplicity, here, we only stress the change of $(220)_{cubic}$. In fact, the $(400)_{cubic}$ and $(422)_{cubic}$ have the same splitting behavior as that of $(220)_{cubic}$ in the annealed and the as-ground samples, respectively.] It reflects a cubic-to-orthorhombic ($P \rightarrow 7M$) transformation at $T_M$. However, in sharp contrast to that, the $(220)_{cubic}$ peak of the as-ground powder sample splits into two peaks $(220)_{tetr}$ and $(202)_{tetr}$, implying a cubic-to-tetragonal ($P \rightarrow 5M$) direct transformation at $T_M$. When the temperature was further lowered down to 150 K, below $T_I$, no change can be found in the XRD pattern of the as-ground powder sample. It implies that the tetragonal ($5M$ martensite) structure remains unchanged during cooling to this temperature range. In contrast to the as-ground powder sample, the XRD pattern of the annealed one shows a remarkable change again at 150 K. Three peaks $(220)_{orth}$, $(202)_{orth}$, and $(022)_{orth}$ changed back to two peaks, i.e., $(220)_{tetr}$ and $(022)_{tetr}$, clearly indicating an orthorhombic-to-tetragonal ($7M \rightarrow 5M$) transformation at $T_I$.

TABLE I. Variation of the average microstrain $\varepsilon$ related to particle size $D$ in the as-ground powder samples. The microstrain $\varepsilon$ values were calculated based on Eq. (1) as discussed in the text.

| Particle size $D$ ($\mu$m) | Microstrain $\varepsilon$ (%) | | |
|---|---|---|---|
| | $\theta_{(220)}$ | $\theta_{(004)}$ | $\theta_{(422)}$ |
| 200–400 | 0.082 | 0.083 | 0.086 |
| 100–200 | 0.292 | 0.289 | 0.295 |
| 50–100 | 0.523 | 0.534 | 0.531 |
| $<50$ | 0.948 | 0.954 | 0.958 |

The XRD experimental data further confirm that the suppression of the intermartensitic transformation in the as-ground powder sample ($D<50$ $\mu$m) should be attributed to the direct transformation from the cubic parent phase $P$ to a $5M$ martensite at $T_M$. That is to say, after grinding the single crystal sample into powders with $D<50$ $\mu$m, the transformation path during cooling will be $P \rightarrow 5M$ completely, instead of the original $P \rightarrow 7M \rightarrow 5M$.

The question arises as to why the as-ground powder and the annealed powder samples undergo completely different structural transformation paths during the martensitic transformation upon cooling. A major difference between the as-ground and the annealed powder samples concerns the condition of the internal stress. From the XRD patterns (see Fig. 3), we observed that the as-ground powder sample has a greater peak broadening. It is well known that the x-ray peak broadening can be caused by both decreasing crystallite size and increasing microstrain. In present work, the contribution of size broadening was negligible because the particle size of our powder is sufficiently large. Therefore, the larger value at the full width at half maximum (FWHM) of XRD reflects the higher microstrain value in the as-ground powder sample. Based on the Scherrer formula,[14] the additional average microstrain $\varepsilon$ in the as-ground powder samples can be written as

$$\varepsilon = \left| \frac{\Delta d}{d} \right| = \frac{\beta}{4 \cdot \tan \theta}, \tag{1}$$

where $d$ is the interplanar spacing, $\theta$ is the Bragg angle, and $\beta = \sqrt{W_1^2 - W_2^2}$. Here, $W_1$ and $W_2$ are the FWHM of corresponding Bragg peaks for the as-ground and the annealed powder samples, respectively, at the parent phase. The calculated results of $\varepsilon$ in the as-ground powder samples with different particle sizes are listed in Table I. The identical values of $\varepsilon$ obtained from different Bragg peaks indicate a clear isotropic microstrain. According to a simple relation,[6] the elastic energy of this material can be evaluated from the

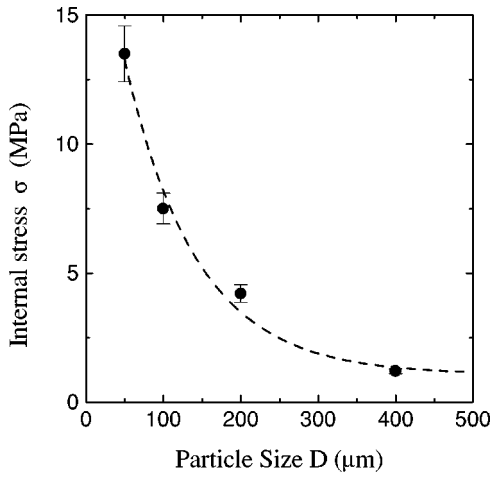


FIG. 4. The calculated average internal stress in the as-ground powder samples as a function of particle size *D*. The dashed line is a least-squares fitting.

value of $\varepsilon$ to yield $E=\frac{1}{2}C\varepsilon^2$, where $C=1.46\times10^{10}$ N/m$^2$ is the bulk Young's modulus.[15] Therefore, in the as-ground powder sample with $D<50$ $\mu$m, the additional average elastic energy is 0.08 J/g. By comparison, it is an order-of-magnitude smaller than the latent heat of the transformation from *P* to $5M$ (1.95 J/g) reported by Vasilev *et al.* in Ref. 12. Therefore, it is reasonable to believe that the as-ground powder samples still keep their parent phase structure at room temperature.

The average internal stress level in the as-ground powder samples was further studied. Figure 4 shows the calculated average internal stress $\sigma(\sigma=C\varepsilon)$ in the as-ground powder samples as a function of particle size *D*. It was found that the average internal stress $\sigma$ increases monotonically with decreasing particle size. In the case of $D<50$ $\mu$m, the average internal stress of $13.8\pm1.08$ MPa is of the same order but less than the threshold external stress value of 35 MPa required to induce $P\rightarrow5M$ martensitic transformation at temperatures above $T_M$.[11] Comparing Fig. 4 and Fig. 2, one can see that the average internal stress of $13.8\pm1.08$ MPa seems to be a critical value for our samples. Larger than this, the two-step $P\rightarrow7M\rightarrow5M$ transformations will switch to a one-step $P\rightarrow5M$ transformation completely during cooling.

We should emphasize that, in the above data analysis, a completely elastic deformation was assumed. Because of the nature of high brittleness of Ni-Mn-Ga alloys in the austenitic state, we believe that the plastic deformation, if any, should be very small and, therefore, may not significantly change the above conclusion. The question of the influence of the plastic deformation on the phase transformation behavior in this material cannot be clearly answered by the present experimental data. In the literature the respective influence of elastic and plastic deformation on the martensitic transformations in lithium metal has been reported,[16] i.e., the elastic deformation facilitates the formation of the low-temperature martensite phase but the plastic deformation will rather suppress it. Viewed in this light, the change of transformation path reported in our present work not only well supports this viewpoint, but strongly suggests that, for Ni-Mn-Ga alloys, the grinding-induced appropriate elastic deformation will facilitate the preferential formation of a $5M$ martensite.

Finally, it is worth pointing out that the average internal stress value of $13.8\pm1.08$ MPa is much less than the external stress level of 35 MPa, and the corresponding elastic energy level of 0.08 J/g is also far from the phase transformation energy of 1.95 J/g. The results suggests that the lowest-energy transformation path between the initial and final states can be alternated by storing appropriate elastic energy in samples. Experimentally such a property has never been investigated and may be useful for the application of Ni-Mn-Ga magnetic shape memory alloys.

In summary, in this paper we have reported the discovery of a *perfect thermoelastic* intermartensitic transformation between the orthorhombic $7M$ and the tetragonal $5M$ martensites in an unstressed $Ni_{52}Mn_{24}Ga_{24}$ single crystal capable of room-temperature martensitic transformation. The obtained experimental results imply that the $7M\rightarrow5M$ intermartensitic transformation of this material is very sensitive to the internal stress built up during the grinding process. Based on our calculation, an average internal stress of $13.8\pm1.08$ MPa stored in the distorted lattice will force the parent phase to take a totally different martensitic transformation path during cooling and results in the complete suppression of the $7M\rightarrow5M$ intermartensitic transformation. It reveals an internal stress-related selectivity of intermartensitic transformation.

This work was supported by the State Key Project of Fundamental Research and the National Natural Science Foundation of China through Grant No. 50131010. G.H.W. and X.X.Z. acknowledge the support of RGC of Hong Kong (Grant No. HKUST6157/00E).

*Author to whom correspondence should be addressed. Email address: userm201@aphy.iphy.ac.cn

[1] K. Ullakko *et al.*, Appl. Phys. Lett. **69**, 1966 (1996).
[2] R. D. James and M. Wuttig, Philos. Mag. A **77**, 1273 (1998).
[3] G. H. Wu *et al.*, Appl. Phys. Lett. **75**, 2990 (1999).
[4] W. H. Wang *et al.*, Appl. Phys. Lett. **77**, 3245 (2000).
[5] W. H. Wang *et al.*, Adv. Eng. Mater. **3**, 330 (2001).
[6] R. C. O'Handley, J. Appl. Phys. **83**, 3263 (1998).
[7] R. Tickle *et al.*, IEEE Trans. Magn. **35**, 4301 (1999).
[8] H. D. Chopra *et al.*, Phys. Rev. B **61**, R14 913 (2000).
[9] Wen-Hong Wang *et al.*, Phys. Rev. B **65**, 012 416 (2002).
[10] A. N. Vasil'ev *et al.*, Phys. Rev. B **59**, 1113 (1999).
[11] V. V. Martynov and V. V. Kokorin, J. Phys. III **2**, 739 (1992).
[12] A. N. Vasilev *et al.*, Pis'ma Zh. Éksp. Teor. Fiz. **58**, 297 (1993) [JETP Lett. **58**, 306 (1993)].
[13] V. A. Chernenko *et al.*, Phys. Rev. B **57**, 2659 (1998).
[14] L. S. Birks and H. Friedman, J. Appl. Phys. **17**, 687 (1946).
[15] J. Worgull *et al.*, Phys. Rev. B **54**, 15 695 (1996).
[16] Ch. Maier *et al.*, Phys. Rev. B **52**, 9283 (1995); **55**, 12 062 (1997); **55**, 113 (1997).